environments

Article

From Waste to Resource: Evaluating Biomass Residues as Ozone-Catalyst Precursors for the Removal of Recalcitrant Water Pollutants

Cátia A. L. Graça [1,2,*] and Olívia Salomé Gonçalves Pinto Soares [1,2]

[1] Laboratory of Separation and Reaction Engineering-Laboratory of Catalysis and Materials (LSRE-LCM), Faculdade de Engenharia, Universidade do Porto, Rua Dr. Roberto Frias, 4200-465 Porto, Portugal; osgps@fe.up.pt
[2] ALiCE—Associate Laboratory in Chemical Engineering, Faculty of Engineering, University of Porto, Rua Dr. Roberto Frias, 4200-465 Porto, Portugal
* Correspondence: catiaalgraca@fe.up.pt

Abstract: Five different biomass wastes—orange peel, coffee grounds, cork, almond shell, and peanut shell—were transformed into biochars (BCs) or activated carbons (ACs) to serve as adsorbents and/or ozone catalysts for the removal of recalcitrant water treatment products. Oxalic acid (OXL) was used as a model pollutant due to its known refractory character towards ozone. The obtained materials were characterized by different techniques, namely thermogravimetric analysis, specific surface area measurement by nitrogen adsorption, and elemental analysis. In adsorption experiments, BCs generally outperformed ACs, except for cork-derived materials. Orange peel BC revealed the highest adsorption capacity (Qe = 40 mg g^{-1}), while almond shell BC showed the best cost–benefit ratio at €0.0096 per mg of OXL adsorbed. In terms of catalytic ozonation, only ACs made from cork and coffee grounds presented significant catalytic activity, achieving pollutant removal rates of 72 and 64%, respectively. Among these materials, ACs made from coffee grounds reveal the best cost/benefit ratio with €0.02 per mg of OXL degraded. Despite the cost analysis showing that these materials are not the cheapest options, other aspects rather than the price alone must be considered in the decision-making process for implementation. This study highlights the promising role of biomass wastes as precursors for efficient and eco-friendly water treatment processes, whether as adsorbents following ozone water treatment or as catalysts in the ozonation reaction itself.

Keywords: biomass waste; carbon materials; catalytic ozonation; cost analysis

Citation: Graça, C.A.L.; Soares, O.S.G.P. From Waste to Resource: Evaluating Biomass Residues as Ozone-Catalyst Precursors for the Removal of Recalcitrant Water Pollutants. *Environments* **2024**, *11*, 172. https://doi.org/10.3390/environments11080172

Academic Editor: Dino Musmarra

Received: 3 July 2024
Revised: 7 August 2024
Accepted: 9 August 2024
Published: 12 August 2024

1. Introduction

Water scarcity is a major concern worldwide since it affects a growing number of regions in the world, year by year. Water reuse, utilizing treated wastewater for non-potable purposes, is one of the multiple strategies that can be adopted to avoid water shortages. However, a fact that discourages a greater adherence to this strategy is the presence of emerging micropollutants in wastewaters, since no or limited regulations and guidelines exist with clear monitoring controls [1]. This fact creates hesitations regarding the reuse of water that may contain these potentially harmful substances. Emerging micropollutants, such as pharmaceuticals and personal care products (PPPCs), appear in wastewater because they are not completely removed by conventional water treatment processes present in most wastewater treatment plants (WWTPs) [2,3], posing unmeasurable threats to aquatic organisms and human health. For instance, Yu et al. (2023) [3] made an ecological risk assessment of the most frequently detected PPPCs in a Chinese river and found out that some are in concentrations with high risk to aquatic organisms (RQ > 1), thus being considered of high-priority concern. Advanced water treatment is thus required to complement WWTPs existing treatments and ensure an efficient removal of this kind of pollutant. In fact, according to the new proposal of the European Union concerning urban wastewater treatment, by

the end of 2035, all urban WWTPs treating a load equal to or greater than 100,000 p.e. would have to provide quaternary treatment to remove a large spectrum of micropollutants [4]. Ozonation has been successfully employed for this purpose in various countries around the world, given the strong oxidizing power of ozone (O_3, E_0 = 2.05 V, NHE) [5], which enables an effective micropollutant abatement and bacteria inactivation [6,7]. However, O_3 presents limited reactivity towards deactivated aromatic or electron-poor aliphatic pollutants [8] under the conditions employed in water treatment, leading to their accumulation in the environment. This is the case of oxalic acid (OXL), a typical ozonation by-product that accumulates due to its refractory character towards O_3 [9]. A possible strategy to remove this kind of refractory by-products would be the combination of an adsorption step after ozonation or the combination of O_3 with catalysts capable of transforming O_3 into more reactive species, such as hydroxyl radicals (•OH, E_0 = 2.8 V, NHE) [10], which are known to be effective against most of O_3-resistant micropollutants [11]. Carbon materials, namely biochars (BCs) and activated carbons (ACs), can act as both adsorbents and O_3 catalysts for the removal of organic compounds [1,12–15]. These are considered more economical and environmentally friendly options than other adsorbents and catalysts used in those processes, since they can be made from inexpensive and 100% natural sources, such as coconut shell [16], or even agricultural and industrial wastes [12,15,17].

This work focuses on developing BCs and ACs derived from 5 different biomass wastes, namely orange peel (OP), coffee ground (CG), cork (CK), almond shell (AS), and peanut shell (PS) and evaluates their potential as both adsorbents and catalysts in the ozonation of OXL. This dual functional approach aims to contribute simultaneously to sustainable waste management and advanced water treatment solutions. These specific 5 biomass wastes were chosen considering their availability in Portugal. Regarding OP, Portugal is a large consumer and producer of oranges, resulting in large quantities of OP waste. Regarding CG, every year in the country's capital Lisbon, 10,000 tonnes of used coffee grounds end up in landfill sites [18]. Regarding CK, Portugal is the largest producer of cork in the world; the country is responsible for over 60% of the volume of all exports [19]. The cork dust that is created when the corks are sanded down to size was the cork waste used in this study. Regarding AS, Portugal is the third-largest almond producer in Europe. As such, AS is the principal byproduct of almond processing and is often considered waste [20]. Finally, PS results from the large consumption of peanuts in Portugal. Although peanuts are grown mainly in Asia, these nuts are the most consumed nuts in Portugal, followed by walnuts [21]. A production cost assessment at laboratory scale of these biomass-derived materials was made to find the material with the best cost-effectiveness ratio, both in terms of OXL removal through adsorption and catalytic ozonation. This aims to be a decision-supporting tool for determining the most economically viable option among the developed materials, a perspective rarely approached in catalytic ozonation studies. Also, although plenty of research is dedicated to repurposing biomass residues into BCs and ACs [17,22–25], their dual role as both adsorbents and O_3 catalysts is still rarely addressed. In fact, only one other study was found exploring this same dual functionality of a biomass-derived carbon material [26], which reinforces the novelty of this study; such an integrated approach is crucial for a sustainable water treatment.

2. Materials and Methods

2.1. Chemicals

The Oxalic acid (OXL, $C_2H_2O_4$, ≥99%) used for the degradation experiments was obtained from Sigma Aldrich (Burlington, MA, USA). Sulphuric acid (H_2SO_4, 95–98%), used as eluent for chromatographic analyses, was also obtained from Sigma Aldrich. All solutions were prepared in ultrapure water (18.2 MΩ·cm), obtained from a Millipore Milli–Q system.

The OP and PS residues were obtained by peeling oranges and peanuts, respectively, which were purchased in local supermarkets. The CK wastes were provided by a cork

producer company located in northern Portugal. The CG was obtained from commercial coffee capsules after usage. The AS was provided by a local farmer.

2.2. Preparation of Biochars (BCs) and Activated Carbons (ACs)

Firstly, the collected biomass residues were submitted to a drying step that consisted of staying in an oven (Thermo Scientific Heraeus UT6120, Cacém, Portugal) at 100 °C overnight (12 h). After this, the dried residues were roughly crushed to better pack inside the furnace reactor.

To produce the biochars, the dried biomass residues were heat-treated under constant N_2 flow (100 cm^3 min^{-1}), at a heating rate of 5 °C min^{-1} until reaching the desired temperature, at which were kept for 1 h (dwell time). To prepare the activated carbons, the dried biomass residues were submitted to one step heat treatment/physical activation route under a constant gas flow of 100 cm^3 min^{-1} containing 30% CO_2 (*w*/*w* %). The heating rate and dwell time were the same as that mentioned for biochars. The dwell temperature was defined based on the thermogravimetric analysis (TGA) of each residue, which is presented ahead in this study. These thermal treatments were performed in a programmable vertical furnace (Termolab, Águeda, Potugal) using a quartz tube reactor.

2.3. Characterization Techniques

The thermogravimetric analyses (TGA) of the samples were performed on a STA 409 PC/4/H Luxx Netzsch thermal analyzer (Netzsch-Gerätebau GmbH, Selb, Germany). The samples were heated at 10 °C min^{-1} under N_2 flow from 50 to 900 °C, then remained at 900 °C for 7 min, followed by 20 min under air flow.

The BET specific surface area and pore size distribution of the produced biochars and activated carbons were evaluated via N_2 adsorption at −196 °C, using a Quantachrome Instruments Nova-e 20200 series (Quantachrome Instruments, Boynton Beach, FL, USA). The specific surface area of the mesoporous (S_{meso}) and the volume of micropores (V_{micro}) were calculated via the t-method using the appropriate standard isotherm; the specific surface area was calculated using the B.E.T. method (S_{BET}), while the average diameter of pores was calculated through the BJH method. Additionally, the total volume of pores was extrapolated from a single point of the adsorption isotherm where p/p_0 = 0.99 ($Vp/p_{0:0.99}$).

Elemental analysis was determined by using an elemental analyzer (Vario Macro Cub, Elementar, Germany).

2.4. Catalytic Ozonation Experiments

To perform the reactions, 50 mg of the prepared BCs or ACs were added to a solution of 100 mL containing 20 mg L^{-1} of OXL. Although OXL is detected in environmental matrices in much lower concentrations (in the order of $\mu g \cdot L^{-1}$), the concentration selected in this study is to guarantee its correct quantification along the degradation studies, considering the limitation of our analytical techniques. The reaction started when a stream of 150 Ncm^3 min^{-1} of O_3 was bubbled into this suspension. The concentration of O_3 in the gas stream was fixed at 50 $g \cdot Nm^3$ by fixing the ozone generator (BMT 802X, BMT MESSTECHNIK GMBH, Stahnsdorf, Germany) power and the pure O_2 flow rate. Adsorption experiments were performed for comparison, replacing the O_3 stream with O_2. Experimental adsorption capacities, Qe (mg g^{-1}), were calculated according to Equation (1).

$$Q_e = \frac{(C_0 - C_e) \cdot V}{W} \quad (1)$$

where C_0 is the initial concentration of OXL, Ce is the OXL concentration at equilibrium time (mg L^{-1}), V is the volume of the OXL solution (L), and W is the mass of the adsorbent (g). The mixture was continuously stirred at 200 rpm, inside a closed stirred tank reactor for 180 min, and aliquots were taken at determined times to quantify OXL concentration. This reactor is equipped with a sampling tube provided with a porous stainless steel filter that allows suspended particles (catalyst) to be separated from the treated solution. A

scheme of the experimental apparatus is shown in our previous publication [1]. Since there could be some fluctuations in the initial OXL concentration, the graphical representation of OXL degradation over time uses the normalized OXL concentration, i.e., $[OXL]/[OXL]_0$ (dimensionless).

2.5. Analytical Methods

The OXL concentration over time was determined via an HPLC–UV (Hitachi Elite LaChrom) (Hitachi, Tokyo, Japan), using an Alltech AO-1000 column (300 mm × 6.5 mm). The isocratic elution for OXL consisted of 100% of an aqueous solution containing 5 mmol·L^{-1} H_2SO_4, at a flow rate of 0.5 mL·min^{-1}. The injection volume was 30 µL, and the detection wavelength was 200 nm. These analytical conditions gave an OXL limit of detection (LOD) of 0.2 mg·L^{-1} and limit of quantification of 0.59 mg·L^{-1}.

3. Results and Discussion

3.1. Characterization of the Prepared Materials

The TGA analyses of the biomass residues are shown in Appendix A (Figures A1–A5 and Table A1). The profile of weight (%) as the temperature (°C) increases presents a stabilization plateau after 400 °C for OP, 600 °C for CK, 500 °C for CG, 400 °C for AS, and 400 °C for PS. Therefore, more thermally stable structures are expected above these temperatures, these having been defined as the setpoint temperatures to convert each biomass residue by pyrolysis and physical activation into BCs and ACs, respectively. These temperatures are in line with other studies where the TGA of the same biomass residue sources were analyzed [15,17,22–25].

Table 1 shows the textural characterization of the prepared BCs and ACs. The BCs present very low surface areas, close to the limit of quantification of the equipment (5 m^2g^{-1}), as well as ACCG. The materials are mostly mesoporous (pores sizes ranging from 50 to 200 Å), except for ACCK, which presents ~74% of microporosity (pore diameter < 20 Å). S_{micro} was calculated from the difference between S_{BET} and S_{meso}. The highest value of surface area (S_{BET}, m^2g^{-1}) was observed for this same material, which can be justified by it being treated at a higher temperature compared to the others.

Table 1. Textural properties of biomass-waste-derived biochar and activated carbons.

Sample	S_{BET} (m^2g^{-1})	S_{meso} (m^2g^{-1})	V_{pores} (p/p_0 = 0.99) (cm^3g^{-1})	Dp BJH (nm)
BCCK	<5	<5	0.01	3.5
BCOP	7	5	0.007	3.5
BCAS	8	4	0.01	4.6
BCPS	<5	<5	0.006	3.7
BCCG	6	<5	0.0001	3.6
ACCK	114	30	0.13	3.7
ACOP	6	<5	0.01	3.5
ACAS	8	6	0.01	3.6
ACPS	53	8	0.04	4.5
ACCG	<5	<5	0.03	3.6

In terms of the elemental composition of the produced materials (Table 2), it is possible to verify a clear decreasing trend in the oxygen content from the biochars to activated carbons from the same biomass source, except for AS, which presents a contrary trend (although very subtle), and CK, where no significant differences can be stated. This may indicate that the physical activation that transformed biochars into activated carbons involved the loss of oxygen-containing functional groups and/or led to more stable structures, i.e., less reactive with the atmospheric O_2 after the thermal treatment, explaining the lower oxygen content in their structures [1,22]. Although the pyrolysis and activation steps occur in the absence of oxygen, partial oxidation might happen due to the inherent oxygen

content in biomass [25], explaining the O % (*w*/*w*) increasing trend observed in the CK- and AS-activated carbons. Considering that carbon content is similar in all the materials and that the O/C ratio is lower in CK and CG-derived materials, less oxygen-containing functional groups are present in the latter, which may influence their stability and reactivity [27]. The H/C ratio always increases from the biochars to activated carbons from the same biomass source, as expected, since during the activation process, there is a consequent removal of carbon atoms, decreasing the carbon content, while the relative proportion of hydrogen-containing functional groups (such as hydroxyl groups, carboxyl groups, and others) increases. Regarding the nitrogen content, it is known that the higher its value, the higher the basicity of the carbon framework, which is known to be beneficial to the catalytic activity against ozone [27,28]. The highest N % [w/t] is observed in the CG-derived materials. Although sulfur (S [%]) was found in vestigial quantities, biochars presented higher values of this element than the activated carbons from the same biomass source, which might contribute to the acidity of the surface and consequent adsorption capacity [29]. Gomes et al. [30] also verified a superior adsorption capacity from sulfur-containing AC towards an organic pollutant over other modified ACs, and the authors attributed this feature to the enhanced affinity that sulfur promotes between the AC surface and the target molecule.

Table 2. Elemental composition of the biomass-derived materials.

Biomass Source		C [%]	H [%]	N [%]	S [%]	O [%]
Orange Peel	Biochar	79.3 ± 22.2	4.7 ± 1.3	1.53 ± 0.2	0.086 ± 0.03	20.47 ± 0.75
	Activated Carbon	70.8 ± 0.6	4.2 ± 0.07	1.5 ± 0.07	0.04 ± 0.01	18.5 ± 0.5
Cork Waste	Biochar	74.35 ± 0.0	2.23 ± 0.0	1.43 ± 0.0	0.02 ± 0.6	9.041 ± 0.5
	Activated Carbon	81.8 ± 1.4	2.5 ± 0.06	1.72 ± 0.03	0	8.49 ± 0.47
Coffee Ground	Biochar	76.9 ± 0.41	3.3 ± 0.04	4.05 ± 0.06	0.033 ± 0.007	12.08 ± 0.13
	Activated Carbon	75.7 ± 0.81	3.33 ± 0.06	4.07 ± 0.07	0.011 ± 0.11	10.34 ± 0.21
Almond Shell	Biochar	77.07 ± 1.26	3.718 ± 0.06	0.01 ± 0.005	0	17.61 ± 1.32
	Activated Carbon	75.83 ± 0.88	3.937 ± 0.05	0.02 ± 0.01	0	20.21 ± 0.50
Peanut Shell	Biochar	81.24 ± 3.34	1.706 ± 0.062	2.59 ± 1.23	0.071 ± 0.013	14.34 ± 0.65
	Activated Carbon	72.44 ± 0.1	4.155 ± 0.044	1.91 ± 0.03	0.053 ± 0.016	11.5 ± 0.3

3.2. Adsorption Experiments

Figure 1 shows the Qe values obtained for all the biomass-derived materials. Except for CK, the biochars revealed a better adsorption capacity than the activated carbons from the same biomass source. Given the polarity of OXL, it is expected that it tends to create more electrostatic interactions with acidic surfaces. According to the elemental analysis in Table 2, biochars are more likely to present a more acidic surface than activated carbons from the same biomass source, explaining this trend. Also, the OP-, AS-, and PS-derived materials are the ones that present more elements of typical acidic functional groups, such as carboxylic acids (-COOH), sulfonic acids (-SO_3H), or phenols (-OH), which also corroborates the higher adsorption capacity observed for these materials [31]. A higher adsorption capacity of the ACCK would be expected, given its superior specific surface area and total volume of pores, but the contrary was observed. A possible explanation would rely on the fact that this material is richer in micropores, which have smaller diameters and might not enable the access of OXL molecules. Also, the surface chemistry can have a more important role than the surface area in the adsorption of OXL by the prepared materials. The adsorption capacity of BCOP outstands all the others, with ~40 mg of OXL adsorbed per g of the BCOP, almost twice the value of that observed with commercial activated carbon (~24 $mg \cdot g^{-1}$). Since OXL is a common ozonation by-product, the adsorption of this contaminant with the BCOP, BCAS, or BCPS after ozone water treatment could be a suitable strategy to avoid OXL accumulation in the treated water.

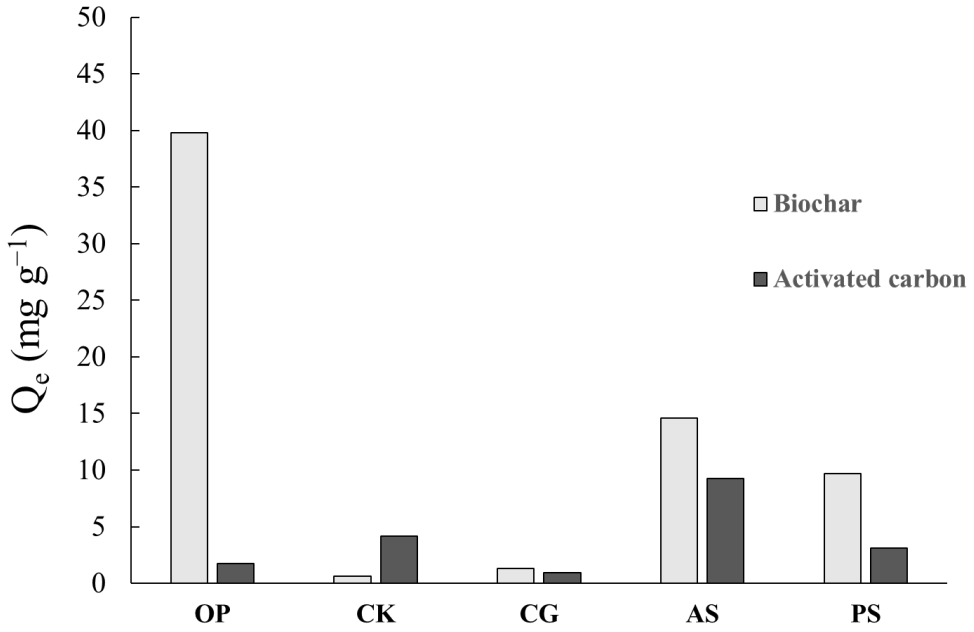

Figure 1. Adsorption capacities Qe (mg g^{-1}).

3.3. Catalytic Ozonation

OXL was selected as a representative of recalcitrant water pollutants since it is a common ozonation by-product of organic pollutants, including pharmaceuticals frequently detected in water bodies [1,32], due to its resistance to ozone [9]. This fact implies that if OXL is well degraded, the prepared materials have successfully catalyzed the transformation of O_3 into hydroxyl radicals (radical pathway).

The degradation profile of OXL promoted by O_3 in the presence of BCs is presented in Figure 2 and in the presence of ACs is presented in Figure 3. It is possible to observe that BCs revealed quite limited catalytic activity, since only the BCAS, BCPS, and BCCK promoted an OXL removal slightly superior to that observed with O_3 alone. Given the more acidic surface predicted for these materials, such an observation is aligned with the established knowledge regarding catalyst activity towards O_3. However, the physical activation of BCCG and BCCK led to materials with increased catalytic activity, as can be observed in the OXL degradation profile promoted by ACCG and ACCK, respectively (Figure 3). Coincidently, these two materials were treated at superior temperatures (500 °C for CG and 600 °C for CK), which means that maybe the other biomass residues would also require higher temperatures during the thermal treatment to become more catalytically active. This suggests further research aiming at optimizing the thermal treatment conditions for each biomass residue in order to convert them in suitable catalysts for ozone-mediated water treatment. Interestingly, the catalytic behavior is the opposite of that observed for adsorption, i.e., the materials with increased catalytic activity are weaker adsorbents of OXL. Probably the superior S_{BET} and V_{pores} of these materials, as well as their surface chemistry (higher N content of ACCG), lead to a faster adsorption of gasses like O_3, thus facilitating the conversion of O_3 into $^{\bullet}OH$ radicals, consequently reflecting in a superior OXL degradation. In fact, there is evidence in the literature that there is a linear correlation between the O_3 decomposition rate and the S_{BET} and pores volume of activated carbons [13].

The OXL degradation profile observed for the BCOP, ACOP, ACAS, and ACPS reveals a loss in the activity of these materials after a certain reaction time. The profile observed in the reaction with these materials is characterized by a first stage of OXL concentration decay, followed by OXL concentration increase back to the initial value. The first OXL decay stage can be explained by the adsorption promoted by these materials, and the second stage can be hypothesized as an OXL desorption from the material surface promoted by a direct O_3 attack or loss of adsorption capacity due to changes in the surface chemistry

also provoked by the O_3 attack [1,33,34]. This behavior also confirms that these materials are not capable of decomposing O_3 into reactive radicals towards OXL, otherwise the OXL concentration would not increase up to its initial value. In sum, ACCK and ACCG were the only biomass-derived materials with a clear capacity for O_3 decomposition and suitable for catalytic ozonation reactions.

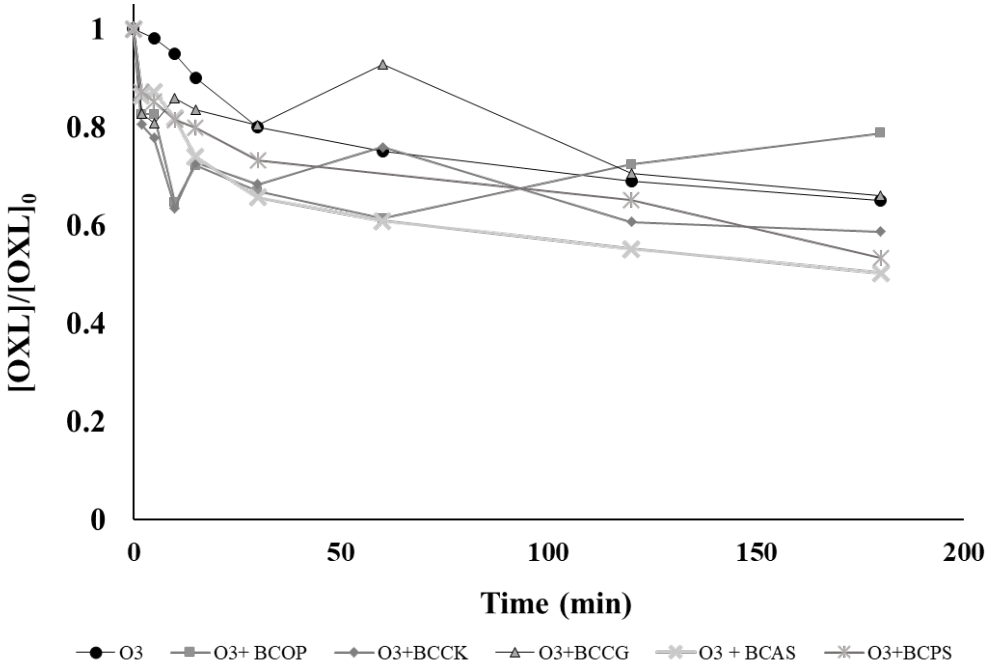

Figure 2. OXL degradation profile promoted by BCs combined with O_3. $[OXL]_0$ = 20 mg·L^{-1}, BCs = 50 mg·L^{-1}, $[O_3]_{gas}$ = 50 g·Nm^3.

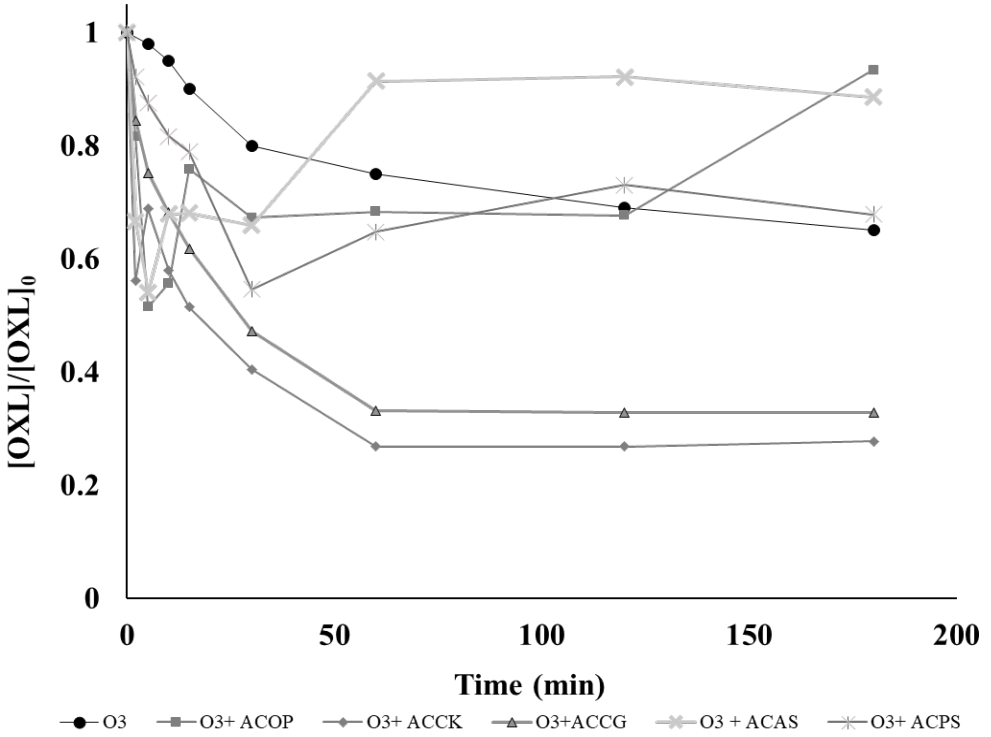

Figure 3. OXL degradation profile promoted by ACs combined with O_3. $[OXL]_0$ = 20 mg·L^{-1}, ACs = 50 mg·L^{-1}, $[O_3]_{gas}$ = 50 g·Nm^3.

3.4. Comparative Cost Analysis

An estimate of the costs associated with the production of BCs and ACs in this study was made, considering the expenses involved with their production at the laboratory scale. The raw biomass was made available at no cost and was the only starting material for BC and ACs production, i.e., no other chemicals were required before submitting the biomass residues to the thermal treatment. The electricity price was adopted as the average wholesale electricity price in Portugal (6.72 €/MWh), and this value was used to calculate the energy costs associated with the energy spent during the drying step and the thermal treatment. The energy consumption per equipment depends on its power. While in the production of the BCs, only N_2 was used, in the production of the Acs, a mixture of N_2:CO_2 70:30 (*w*/*w*) was used in the gas stream; thus, the price of consumption of these gasses was calculated, considering the total volume of gas spent in one batch treatment. Based on the gas cylinders prices made available by the suppliers, these gasses are priced as 2.5 €/m^3 for N_2 and 3.4 €/m^3 for CO_2. After the thermal treatment per se, these gasses continue being consumed during the cool-down stage, the duration of which varies according to the final dwell temperature, i.e., the higher the dwell temperature, the more it takes to reach the ambient temperature. Only when the ambient temperature is reached are the gasses turned off, and the treatment is finished.

The mass of biomass residue that fits into the furnace reactor depends on its nature and the yield of conversion of this biomass into BCs and ACs also; therefore, these aspects were also taken into account in calculating the production costs. The input mass per production batch was 2 g for the orange peels, 1.5 g for the cork, 2 g for the coffee grounds, 15 g for the almond shells, and 7 g for the peanut shells. These masses represent similar volumes that fit into the furnace reactor. The yields of conversion of these biomass residues into BCs and ACs were considered for a more accurate cost estimation. Appendix B has the input data considered in the calculation of the final production cost of each material (€/g). Solely considering the final value, it can be concluded that AS is the residue that produces the cheapest materials, with 0.14 and 0.13 €/g for BCAS and ACAS, respectively. This is justified by the fact that AS, due to its density, enables treating a higher mass per batch. Thus, even though not presenting the highest yield, a greater amount of BC and AC are produced with this residue, decreasing the cost of production per batch.

To have a more accurate comparison between the materials, a cost ratio indicator was calculated considering the total price of production of each material (Tables A2 and A3, Appendix B) divided by the mass of OXL adsorbed or the % of OXL removed by catalytic ozonation. Table 3 shows the cost ratios calculated for each biomass-derived carbon material and also includes the values obtained with a commercial version of granular-activated carbon tested in a previous work [1], for the sake of comparison. This commercial AC presents a cost of 0.13 €/g, quite close to that obtained for ACAS.

Considering the adsorption process, none of the developed materials presents a lower cost ratio than that observed with the commercial AC (0.00525 €/g OXL removed). Among the biomass-derived materials, BCAS presents the lowest cost ratio (0.0096 €/mg of OXL adsorbed). This can be explained by the fact that this is among the materials with the cheapest production cost, which presents a higher adsorption capacity (the second highest Qe of 14.62 mg OXL adsorbed/g of BCAS). Coincidentally, this is also the most economic material to carry out the catalytic ozonation reaction, with a cost ratio of 0.003 €/% of OXL removed by catalytic ozonation, quite close to that of commercial AC (0.002 €/% of OXL removed by catalytic ozonation). However, BCAS presents limited catalytic activity. Focusing only on the best-performing material for the catalytic ozonation process in terms of OXL % removal, ACCG presents the cheapest option, with a cost ratio of 0.02 €/% of OXL removed. These results demonstrate that choosing a catalyst for a particular reaction involves a comprehensive evaluation that considers multiple factors, rather than based solely on one aspect, such as catalytic activity or cost. While for adsorption it seems clear that BCAS presents the best balance between activity and cost-effectiveness, for catalytic ozonation, this is not so straightforward. For the latter, other aspects must also be

considered in future studies, such as durability and stability of the catalyst in continuous or long-term reactions.

Table 3. Cost ratios based on adsorption and catalytic ozonation performances of each material.

	Adsorption		Catalytic Ozonation	
Biomass-Derived Carbon Material	**Q_e (mg/g)**	**Cost Ratio Adsorption (€ Adsorbent/mg OXL Removed)**	**% OXL Removed in 180 min**	**Cost Ratio Catalysis (€ Catalyst/% OXL Removed)**
BCOP	39.82	0.023	21	0.04
BCCK	0.63	3.90	41	0.06
BCCG	1.33	1.38	34	0.05
BCAS	14.62	0.0096	49.8	0.003
BCPS	9.69	0.031	46.6	0.006
ACOP	1.74	0.51	7	0.13
ACCK	4.19	0.53	72	0.03
ACCG	0.932	1.44	67.3	0.02
ACAS	9.28	0.014	0	n.d.
ACPS	3.14	0.084	32.2	0.008
Commercial Granular-Activated Carbon	24	0.00525	63	0.002

n.d. stands for "not determined".

4. Conclusions

BCs and ACs made from 5 different biomass sources, namely OP, CK, CG, AS, and PS, were prepared to be used as potential adsorbents and/or catalysts in an ozonation reaction for the abatement of recalcitrant water pollutants. The results showed that the BCs made from OP (BCOP), AS (BCAS), and PS (BCPS) were effective in the adsorption of the model pollutant, OXL, with BCAS representing the cheapest production and process cost (0.14 €/g of BCAS produced and 0.0096 €/mg of OXL adsorbed with BCAS). However, the BCs did not reveal significant catalytic activity when coupled to O_3, their application only being suitable if an adsorption step is employed after an ozone water treatment for the removal of ozone-resistant by-products. The ACs made from CK and CG (ACCK and ACCG, respectively) were the only materials with significant catalytic activity towards O_3, which was attributed to their textural properties and surface chemistry. However, these materials present a catalytic cost ratio of 0.03 and 0.02 € per % OXL removed by catalytic ozonation, respectively, thus not representing the cheapest options. The comparative laboratory cost analysis performed to estimate these cost ratios enabled concluding that the most effective material in terms of OXL removal, both by adsorption and catalytic ozonation, does not necessarily represent the most economical solution. In terms of adsorption, BCAS is clearly the most appropriate option with the best cost/benefit ratio, but this is not so straightforward for catalytic ozonation. Nevertheless, this cost estimation provided useful insights into the overall feasibility of the developed materials for practical application. Some other relevant aspects to assess the real applicability of these biomass-derived materials include the evaluation of their adsorption and catalytic performance in real water matrices, as well as their reusability, which will be the focus of future work. Notwithstanding, the results of this study provide new possibilities for the use of biomass residues and encourage future research to optimize their potential for the removal of ozone-recalcitrant pollutants from water.

Author Contributions: Conceptualization, C.A.L.G. and O.S.G.P.S.; methodology, C.A.L.G. and O.S.G.P.S.; validation, O.S.G.P.S.; formal analysis, C.A.L.G. and O.S.G.P.S.; investigation, C.A.L.G.; resources, C.A.L.G. and O.S.G.P.S.; writing—original draft preparation, C.A.L.G.; writing—review and editing, O.S.G.P.S.; supervision, O.S.G.P.S.; project administration, O.S.G.P.S.; funding acquisition, C.A.L.G. and O.S.G.P.S. All authors have read and agreed to the published version of the manuscript.

Funding: This work was supported by national funds through FCT/MCTES (PIDDAC): LSRE-LCM, UIDB/50020/2020 (DOI: 10.54499/UIDB/50020/2020) and UIDP/50020/2020 (DOI: 10.54499/UIDP/50020/2020); and ALiCE, LA/P/0045/2020 (DOI: 10.54499/LA/P/0045/2020). C.A.L. Graça thanks FCT funding under the Scientific Employment Stimulus—Individual Call 2022.08029.CEECIND (DOI: 10.54499/2022.08029.CEECIND/CP1733/CT0010). O.S.G.P. Soares thanks FCT funding under the Scientific Employment Stimulus—Institutional Call CEEC-INST/00049/2018 ((DOI: 10.54499/CEECINST/00049/2018/CP15 24/CT0008).

Data Availability Statement: The data presented in this study are available upon demand from the correspondence author.

Conflicts of Interest: The authors declare no conflicts of interest.

Appendix A. TGA and DTG Curves of Biomass Residues

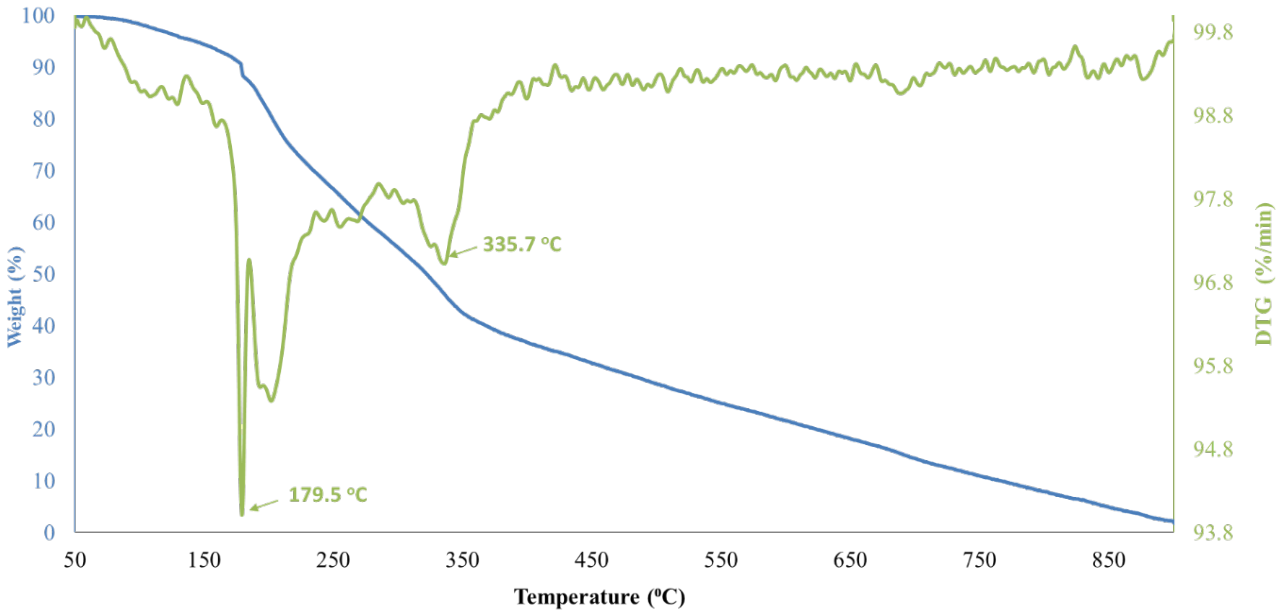

Figure A1. TGA and DTG curves for orange peel.

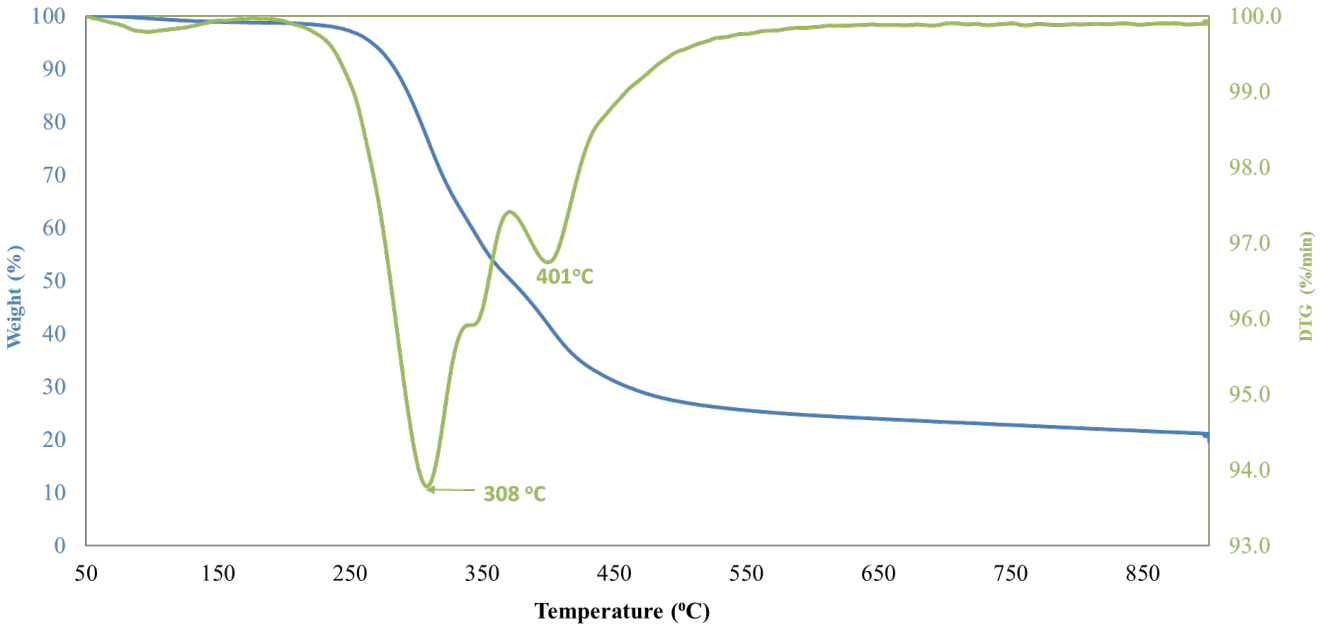

Figure A2. TGA and DTG curves for coffee ground.

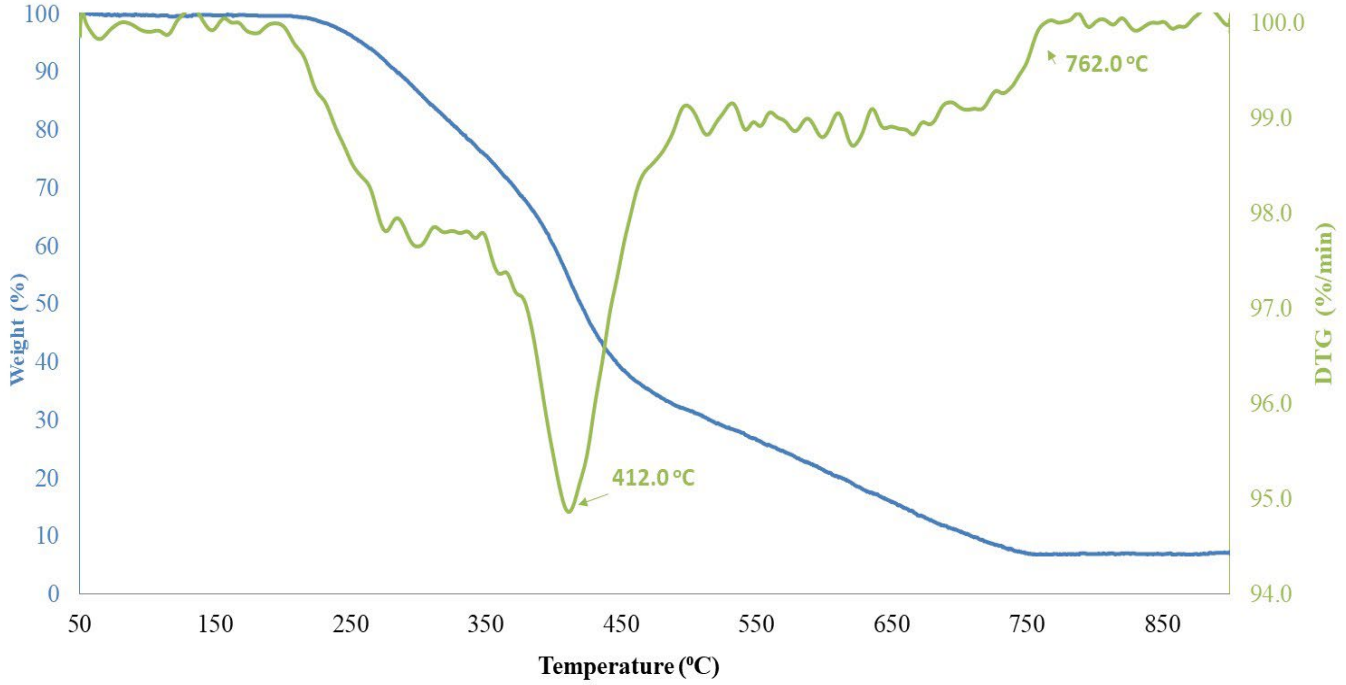

Figure A3. TGA and DTG curves for cork waste.

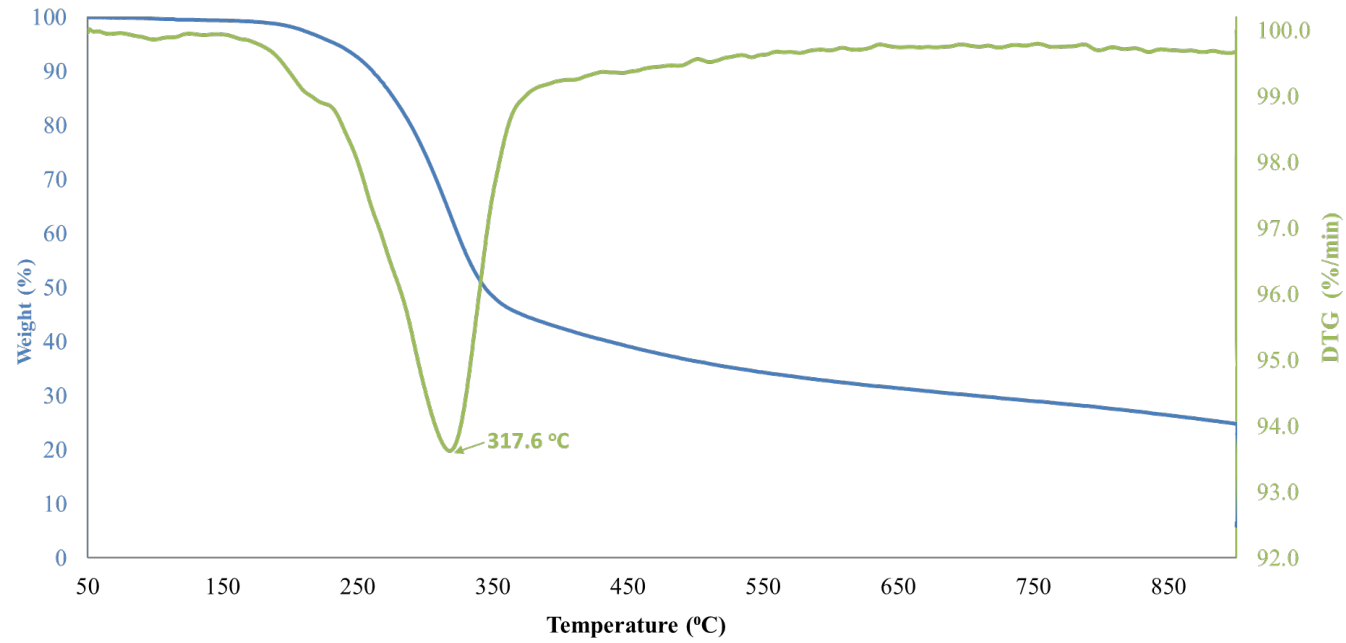

Figure A4. TGA and DTG curves for almond shell.

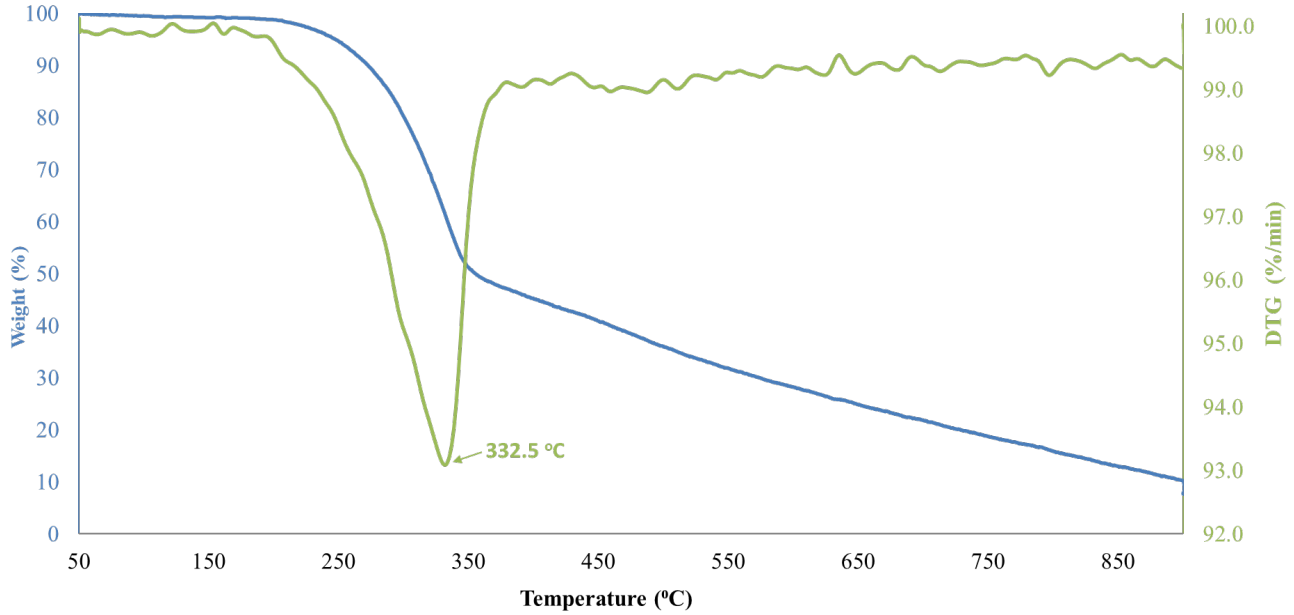

Figure A5. TGA and DTG curves for peanut shell.

Table A1. Proximate analysis of the biomass residues.

Biomass Source	Volatile Matter (wt. % Dry Basis)	Fixed Carbon (wt. % Dry Basis)	Ash (wt. %)
Orange Peel (OP)	99.7	0.3	0.6
Cork Waste (CK)	93.2	0.0	6.8
Coffee Ground (CG)	79.8	1.0	19.2
Almond Shell (AS)	77.4	16.9	5.7
Peanut Shell (PS)	92.8	0.1	7.1

Appendix B. Data Used for the Cost Analysis

Table A2. Input data for the calculation of the production cost of the biomass-derived materials.

Power Muffle	6.1	Kwatts
Power Furnace	4.8	Kwatts
Average Energy Price	0.00672	€/KWH
Price N_2	0.0025	€/L
Price CO_2	0.0034	€/L

Table A3. Estimation of the production costs for the biomass-derived materials.

Carbon Materials	Drying Time (min)	Pyrolysis + Activation Time (min)	Cool-Down Time (min)	€ Gases	Price Electricity €	Production Yield (%)	Output g/Batch	Cost/Batch (€/g)
BCOP	720	140	120	0.065	0.567	0.34	0.68	0.930
BCCK	720	180	120	0.075	0.589	0.18	0.27	2.458
BCCG	720	160	180	0.085	0.578	0.18	0.36	1.841
BCAS	720	140	120	0.065	0.567	0.3	4.5	0.140
BCPS	720	200	180	0.095	0.599	0.33	2.31	0.301
ACOP	720	140	120	0.07	0.567	0.36	0.72	0.888
ACCK	720	180	120	0.08	0.589	0.2	0.3	2.239
ACCG	720	160	180	0.09	0.578	0.25	0.5	1.344
ACAS	720	140	120	0.07	0.567	0.32	4.8	0.133
ACPS	720	200	180	0.11	0.599	0.38	2.66	0.265

References

1. Graca, C.A.L.; Zema, R.; Orge, C.A.; Restivo, J.; Sousa, J.; Pereira, M.F.R.; Soares, O.S.G.P. Temperature and nitrogen-induced modification of activated carbons for efficient catalytic ozonation of salicylic acid as a model emerging pollutant. *J. Environ. Manag.* **2023**, *344*, 118639. [CrossRef] [PubMed]
2. Paíga, P.; Correia, M.; Fernandes, M.J.; Silva, A.; Carvalho, M.; Vieira, J.; Jorge, S.; Silva, J.G.; Freire, C.; Delerue-Matos, C. Assessment of 83 pharmaceuticals in WWTP influent and effluent samples by UHPLC-MS/MS. *Sci. Total Environ.* **2019**, *648*, 582–600. [CrossRef]
3. Yu, X.P.; Yu, F.R.; Li, Z.P.; Zhan, J. Occurrence, distribution, and ecological risk assessment of pharmaceuticals and personal care products in the surface water of the middle and lower reaches of the Yellow River (Henan section). *J. Hazard. Mater.* **2023**, *443*, 130369. [CrossRef]
4. European Commission. Proposal for a Directive of the European Parliament and of the Council Concerning Urban Wastewater Treatment (Recast). EUR-Lex. 2022. Available online: https://eur-lex.europa.eu/legal-content/EN/TXT/?uri=CELEX:52022PC0541 (accessed on 30 July 2024).
5. Deng, Y.; Zhao, R.Z. Advanced Oxidation Processes (AOPs) in Wastewater Treatment. *Curr. Pollut. Rep.* **2015**, *1*, 167–176. [CrossRef]
6. Graça, C.A.L.; Ribeirinho-Soares, S.; Abreu-Silva, J.; Ramos, I.I.; Ribeiro, A.R.; Castro-Silva, S.M.; Segundo, M.A.; Manaia, C.M.; Nunes, O.C.; Silva, A.M.T. A Pilot Study Combining Ultrafiltration with Ozonation for the Treatment of Secondary Urban Wastewater: Organic Micropollutants, Microbial Load and Biological Effects. *Water* **2020**, *12*, 3458. [CrossRef]
7. Lim, S.; Shi, J.L.; von Gunten, U.; McCurry, D.L. Ozonation of organic compounds in water and wastewater: A critical review. *Water Res.* **2022**, *213*, 118053. [CrossRef]
8. Kasprzyk-Hordern, B.; Ziólek, M.; Nawrocki, J. Catalytic ozonation and methods of enhancing molecular ozone reactions in water treatment. *Appl. Catal. B—Environ.* **2003**, *46*, 639–669. [CrossRef]
9. Gonçalves, A.G.; Orfao, J.J.M.; Pereira, M.F.R. Ozonation of bezafibrate over ceria and ceria supported on carbon materials. *Environ. Technol.* **2015**, *36*, 776–785. [CrossRef] [PubMed]
10. Cretin, M.; LE, T.X.H. •OH Radicals Production. In *Encyclopedia of Membranes*; Drioli, E., Giorno, L., Eds.; Springer: Berlin/Heidelberg, Germany, 2015; pp. 1–2.
11. López-Francés, A.; Bernat-Quesada, F.; Cabrero-Antonino, M.; Ferrer, B.; Dhakshinamoorthy, A.; Baldoví, H.G.; Navalón, S. Nanographite: A highly active and durable metal-free ozonation catalyst with application in natural waters. *Appl. Catal. B* **2023**, *336*, 122924. [CrossRef]
12. Jaria, G.; Silva, C.P.; Oliveira, J.; Santos, S.M.; Gil, M.V.; Otero, M.; Calisto, V.; Esteves, V.I. Production of highly efficient activated carbons from industrial wastes for the removal of pharmaceuticals from water-A full factorial design. *J. Hazard. Mater.* **2019**, *370*, 212–218. [CrossRef] [PubMed]
13. Faria, P.C.C.; Orfäo, J.J.M.; Pereira, M.F.R. Ozone decomposition in water catalyzed by activated carbon: Influence of chemical and textural properties. *Ind. Eng. Chem. Res.* **2006**, *45*, 2715–2721. [CrossRef]
14. Liu, Z.Q.; Li, J.Y.; Li, S.T. Catalytic Ozonation over Activated Carbon-based Materials. In *Advanced Ozonation Processes for Water and Wastewater Treatment: Active Catalysts and Combined Technologies*; Cao, H., Xie, Y., Wang, Y., Xiao, J., Eds.; The Royal Society of Chemistry: London, UK, 2022; pp. 85–122.
15. Li, H.; Liu, S.; Qiu, S.; Sun, L.; Yuan, X.; Xia, D. Catalytic ozonation oxidation of ketoprofen by peanut shell-based biochar: Effects of the pyrolysis temperatures. *Environ. Technol.* **2022**, *43*, 848–860. [CrossRef] [PubMed]
16. Brito, G.M.; Roldi, L.L.; Schetino, M.A., Jr.; Checon Freitas, J.C.; Cabral Coelho, E.R. High-performance of activated biocarbon based on agricultural biomass waste applied for 2,4-D herbicide removing from water: Adsorption, kinetic and thermodynamic assessments. *J. Environ. Sci. Health B* **2020**, *55*, 767–782. [CrossRef] [PubMed]
17. Debevc, S.; Weldekidan, H.; Snowdon, M.R.; Vivekanandhan, S.; Wood, D.F.; Misra, M.; Mohanty, A.K. Valorization of almond shell biomass to biocarbon materials: Influence of pyrolysis temperature on their physicochemical properties and electrical conductivity. *Carbon Trends* **2022**, *9*, 100214. [CrossRef]
18. Portugal Startups. From Waste to Taste: Growing Mushrooms from Recycled Coffee Grounds. Portugal Startups. Available online: https://portugalstartups.com/2019/11/from-waste-to-taste-growing-mushrooms-from-recycled-coffee-grounds/ (accessed on 30 July 2024).
19. Visit Portugal. The Cork. Available online: https://www.visitportugal.com/en/content/the-cork (accessed on 30 July 2024).
20. Campos, C.R.; Sousa, B.; Silva, J.; Braga, M.; Araújo, S.d.S.; Sales, H.; Pontes, R.; Nunes, J. Positioning Portugal in the context of world almond production and research. *Agriculture* **2023**, *13*, 1716. [CrossRef]
21. Guiné, R.P.F.; Correia, P.; Fernandes, S.; Ramalhosa, E. Consumption of nuts and similar dried foods in Portugal and level of knowledge about their chemical composition and health effects. *J. Nuts.* **2021**, *12*, 171–200.
22. Akhil, D.; Lakshmi, D.; Kartik, A.; Vo, D.V.N.; Arun, J.; Gopinath, K.P. Production, characterization, activation and environmental applications of engineered biochar: A review. *Environ. Chem. Lett.* **2021**, *19*, 2261–2297. [CrossRef]
23. Kwon, D.; Oh, J.I.; Lam, S.S.; Moon, D.H.; Kwon, E.E. Orange peel valorization by pyrolysis under the carbon dioxide environment. *Bioresource Technol.* **2019**, *285*, 121356. [CrossRef] [PubMed]

24. Mukherjee, A.; Saha, B.; Niu, C.; Dalai, A.K. Preparation of activated carbon from spent coffee grounds and functionalization by deep eutectic solvent: Effect of textural properties and surface chemistry on CO_2 capture performance. *J. Environ. Chem. Eng.* **2022**, *10*, 108815. [CrossRef]
25. Sen, A.U.; Fonseca, F.G.; Funke, A.; Pereira, H.; Lemos, F. Pyrolysis kinetics and estimation of chemical composition of cork. *Biomass Convers. Bior.* **2022**, *12*, 4835–4845. [CrossRef]
26. Francoeur, M.; Yacou, C.; Petit, E.; Granier, D.; Flaud, V.; Gaspard, S.; Brosillon, S.; Ayral, A. Removal of antibiotics by adsorption and catalytic ozonation using magnetic activated carbons prepared from *Sargassum* sp. *J. Water Process Eng.* **2023**, *53*, 103602. [CrossRef]
27. Hagemann, N.; Spokas, K.; Schmidt, H.P.; Kägi, R.; Böhler, M.A.; Bucheli, T.D. Activated Carbon, Biochar and Charcoal: Linkages and Synergies across Pyrogenic Carbon's ABCs. *Water* **2018**, *10*, 182. [CrossRef]
28. Bakshi, S.; Banik, C.; Laird, D.A. Estimating the organic oxygen content of biochar. *Sci. Rep.* **2020**, *10*, 13082. [CrossRef]
29. Villalgordo-Hernández, D.; Grau-Atienza, A.; García-Marín, A.A.; Ramos-Fernandez, E.V.; Narciso, J. Manufacture of Carbon Materials with High Nitrogen Content. *Materials* **2022**, *15*, 2415. [CrossRef] [PubMed]
30. Gomes, H.T.; Miranda, S.M.; Sampaio, M.J.; Silva, A.M.T.; Faria, J.L. Activated Carbons treated with sulphuric acid: Catalysts for catalytic wet peroxide oxidation. *Catal. Today* **2010**, *151*, 153–158. [CrossRef]
31. Rocha, R.P.; Restivo, J.; Sousa, J.P.S.; Orfao, J.J.M.; Pereira, M.F.R.; Figueiredo, J.L. Nitrogen-doped carbon xerogels as catalysts for advanced oxidation processes. *Catal. Today* **2015**, *241*, 73–79. [CrossRef]
32. Petit, C.; Peterson, G.W.; Mahle, J.; Bandosz, T.J. The effect of oxidation on the surface chemistry of sulfur-containing carbons and their arsine adsorption capacity. *Carbon* **2010**, *48*, 1779–1787. [CrossRef]
33. Orge, C.A.G.; Graça, C.A.L.; Restivo, J.; Pereira, M.F.R.; Soares, O.S.G.P. Catalytic ozonation of pharmaceutical compounds using carbon-based catalysts. *Catal. Commun.* **2024**, *187*, 106863. [CrossRef]
34. Santos, A.S.G.G.; Orge, C.A.; Soares, O.S.G.P.; Pereira, M.F.R. 4-Nitrobenzaldehyde removal by catalytic ozonation in the presence of CNT. *J. Water Process Eng.* **2020**, *38*, 101573. [CrossRef]